CFD Letters

Journal homepage:
https://semarakilmu.com.my/journals/index.php/CFD_Letters/index
ISSN: 2180-1363

Entropy Generation of Three-Dimensional Williamson Nanofluid Flow Explored with Hybrid Carbon Nanotubes over a Stretching Sheet

P. S. S. Nagalakshmi[1], N. Vijaya[1,*], Shaik Mohammed Ibrahim[1]

[1] Department of Engineering Mathematics, College of Engineering, Koneru Lakshmaiah Education Foundation, Vaddeswaram, Andhra Pradesh 522302, India

ARTICLE INFO

Article history:
Received 14 August 2022
Received in revised form 13 September 2022
Accepted 14 October 2022
Available online 1 July 2023

Keywords:
Python; Hybrid CNT; Peclet number

ABSTRACT

The current study simulated the three-dimensional Williamson nanofluid flow model over a stretching sheet in the presence of Cason parameter explored with hybrid carbon nanotubes. The governing equations are modelled and interpreted using adequate similarity transformations and physical phenomena to convert into nonlinear coupled ordinary differential equations. In order to solve these equations, a Python coding program is used with an open-source boundary value problem solver. The obtained numerical results are validated with related literature results. The results are interpreted through graphs and tables with thermos-physical parameters like thermal Peclet number. It is found that the growth rate of heat transfer from fluid to wall with booming non-linear thermal radiation, radiation, and thermal Peclet number parameters.

1. Introduction

In the recent trend, high thermal conductive fluids such as nanofluids have been dominated in heat and mass transfer systems. It's common to suspend nanoparticles (10nm or smaller) in a base fluid, such as water, in the same manner as water dissolves particles. Fluids commonly used for nanoparticle suspension include engine oil, kerosene, and ethanol. In some engineering, biomedical, and industrial fields, this colloidal mixture can improve nano liquid's thermal conductivity for heat transport considerations. Since 1995, Choi has been developing nano fluids. There has been a great deal of research in the past few years that has studied the properties of nanofluids, including their heat and mass transfer capabilities. Numerical solutions for the porous medium problem of flow are studied in relationship to chemical reaction parameters and fluid properties are taken from g to Modather *et al.,* [1]. Adopting the control-volume-based finite element method (CVFEM), the shape of nanoparticles was numerically analyzed to determine their impact on rate of heat transfer and their correlation with the thermophysical parameters of nanofluids are carried out from Chamkha *et al.,* [2]. Flow intensity varies inversely with the Hartmann number and magnetic field inclination angle, while it is directly proportional to Rayleigh and Darcy numbers are analyzed by Dogonchi *et*

* *Corresponding author.*
E-mail address: vijayanalleboyina@kluniversity.in (N. Vijaya)

https://doi.org/10.37934/cfdl.15.7.112130

al., [3]. In terms of suction and chemical reaction parameters, the thermal and mass transfer coefficients of nanofluids (Ag and TiO_2) are calculated are studied by Krishna and Chamkha [4]. A temperature and concentration profile of nanofluid flow is examined based on Brownian motion and thermophoresis are computed from Krishna and Chamkha [5]. The skin friction coefficient of nanofluids undergoing magnetohydrodynamic (MHD) free convective rotating flow over a moving semi-infinite flat plate was studied by examining the Hall and ion slip parameters are taken from Krishna and Chamkha [6]. Unsteady magnetohydrodynamic (MHD) rotating flow over a saturated porous medium, magnetic field and angle of inclination were examined to determine engineering coefficients of heat and mass transfer are examined by Krishna *et al.,* [7]. Thermal energy transfer of natural convection nanofluid flow within a crown cavity with a circular cylinder inside building the cause-and-effect relationship among thermophysical parameters, Nusselt number, and entropy generation was computed by Dogonchi *et al.,* [8]. In a porous enclosure with two square cylinders, the Hartmann number and mount Rayleigh number were observed as they affected the generation of entropy in magnetic Fe_3O_4-H_2O nanofluid flow are taken from Dogonchi *et al.,* [9]. Jeffery Hamel flow with suction and injection using homotopy analysis method is solved from Hamrelaine *et al.,* [10]. Impact of heat source parameter with local Nusselt and Sherwood number of micro polar fluids are studied from Khan *et al.,* [11].

Non-Newtonian fluids are predominantly composed of pseudoplastic fluids or shear-thinning fluids. A wide variety of industries benefit is identified from the study of shear-thickening fluid boundary layers. These applications include extrusion of polymer sheets, coating of photographic films, simulations, melting of high-mass polymers, colloidal suspensions, molten polymers, and building materials. Williamson proposed an equation in 1929 to describe the flow of pseudoplastic materials. The Williamson fluid flow on an inclined surface under the influence of a gravitational field was studied by Lyubimov and Perminov in 2002. Heat transfer model for Williamson fluid over exponentially stretching surfaces are explained by Nadeem and Hussain [12]. The impacts of thermal radiation on particle-liquid suspensions of Williamson fluid are examined from Kumar *et al.,* [13]. Numerical simulations of slippage over a vertical convection surface in an MHD Williamson fluid flow are described from Amanulla *et al.,* [14]. MHD flow of Williamson fluid with slippage has a dual solution are studied from Lund *et al.,* [15]. Williamson nanofluid thermal and velocity slips using the Buongiorno thermal and mass transfer model are examined from Kho *et al.,* [16]. Researchers investigated how binary chemical reactions generate Entropy in Darcy–Forchheimer Williamson nanofluids flowing over non-linearly stretching surfaces are computed from Rasool *et al.,* [17]. Modeling and studying the flow of Williamson nanofluid over nonlinear stretching plates with activation energy are analyzed from Dawar *et al.,* [18]. An analysis of Williamson nanofluid heat transfer under MHD is presented by Qureshi [19]. Thermal boundary layer and coefficient of Nusselt number were examined by Williamson fluid flow over a stretching sheet with Newtonian heating are computed from Goud [20]. An exponentially stretching surface is the basis for a numerical study of magnetohydrodynamic Williamson nanofluid flow is taken from Ahmed and Akbar [21].

Nanoparticle constructions offer superior structural properties, coatings and paints with functional properties, and high-resolution sensing and actuation devices. A cylindrical structure, carbon nanotubes (CNTs) possess irreplaceable properties, such as superior thermal conductivity and incredible power. Their versatility makes them highly desirable materials for various purposes, such as microwave amplifiers, optics, drug delivery, nanotube transistors, prosthetics, etc. Depending on how they are manufactured, carbon nanotubes can either be single-wall carbon nanotubes (SWCNTs) or multi-wall carbon nanotubes (MWCNTs). The MWCNT was developed by Iijima in 1991. Donald Bethune came up with the idea of SWCNTs in 1993. Adding CNTs to polymeric chemical admixtures can improve mechanical strength by gluing concrete mixtures and preventing crack propagation.

Nondecorative ceramics become more resistant to heat and scratch damage when CNTs are used to improve their thermal properties. Recent research has shown that hybrid nanofluids consisting of suspended carbon nanotubes have overcome the disadvantages of mono nanofluids.

Numerous papers address nanofluids with varied geometries. However, there is no such study like the adopted study in the presence of thermal Peclet number to observe the deformation of Williams 'nanofluids utilizing hybrid carbon nanotubes on stretched sheets near the boundary layer. Further, this exploration becomes unique when the above-mentioned characteristics are supported with nano thermophysical properties of hybrid carbon nanotubes explored with SWCNT and MWCNT. Numerical results for the erected model are obtained by using a built-in Python function with BVP.

2. Mathematical Formulation

The researchers are exploring a three-dimensional flow of incompressible nanofluid using hybrid CNTs. The flow is induced by stretching sheets at z=0 (see Figure 1). Suppose the plate is maintained in the XY plane with z=0 and that the flow occurs in the z> 0 domain. Let $p=p_w$, $q=q_w$, $T=T_w$, and $C=C_w$ be the velocities, temperature, and concentration of the nanofluid near the surface of the stretching sheet. Moreover, investigators assume that the rheological state of an incompressible Williamson's nanofluid with Cason effect can be written as [21]

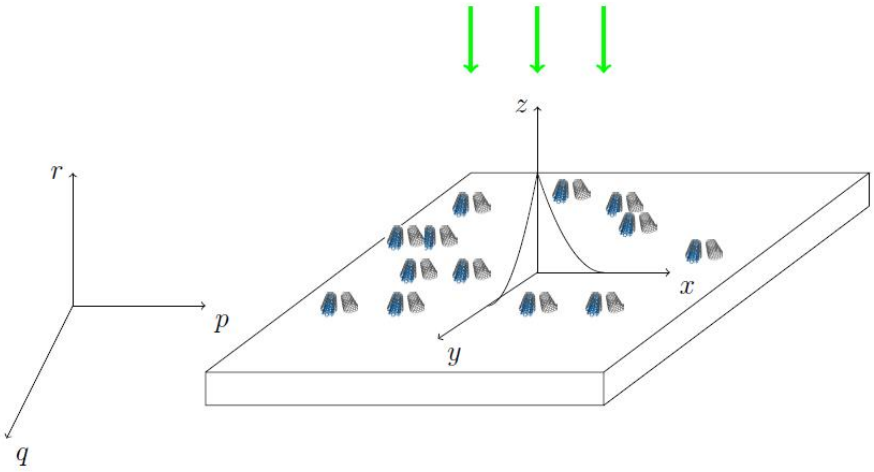

Fig. 1. Flow diagram

$$\frac{\partial p}{\partial x}+\frac{\partial q}{\partial y}+\frac{\partial r}{\partial z}=0, \tag{1}$$

$$p\frac{\partial p}{\partial x}+q\frac{\partial p}{\partial y}+r\frac{\partial p}{\partial z} = \nu_{hnf}\left(1+\frac{1}{\beta}\right)\frac{\partial^2 p}{\partial z^2}+\sqrt{2}\tau\nu_{hnf}\frac{\partial p}{\partial z}\frac{\partial^2 p}{\partial z^2}-\sigma_{hnf}\frac{B^2}{\rho_{hnf}}p, \tag{2}$$

$$p\frac{\partial q}{\partial x}+q\frac{\partial q}{\partial y}+r\frac{\partial q}{\partial z} = \nu_{hnf}\left(1+\frac{1}{\beta}\right)\frac{\partial^2 q}{\partial z^2}+\sqrt{2}\tau\nu_{hnf}\frac{\partial q}{\partial z}\frac{\partial^2 q}{\partial z^2}-\sigma_{hnf}\frac{B^2}{\rho_{hnf}}q, \tag{3}$$

$$p\frac{\partial T}{\partial x}+q\frac{\partial T}{\partial y}+r\frac{\partial T}{\partial z} = \frac{k_{hnf}}{(\rho c_p)_{hnf}}\frac{\partial^2 T}{\partial z^2}+\frac{D_T}{T_\infty}\left(\frac{\partial T}{\partial z}\right)^2+\frac{16\sigma^*}{3k^*}\frac{\partial}{\partial z}\left(T^3\frac{\partial T}{\partial z}\right). \tag{4}$$

Boundary conditions [21]

$$p = p_w = p_0 e^{\frac{x+y}{l}}, q = q_w = q_0 e^{\frac{x+y}{l}}, r = 0,$$
$$-k_{hnf}\frac{\partial T}{\partial z} = (\rho c_p)_{hnf} p_w (T_w - T), as\ z \to 0 \quad (5)$$
$$p \to 0, q \to 0, r \to 0, T \to T_\infty, as\ z \to \infty.$$

Here, as in the above formulas and derivation the values such as p, q, and r are velocity components in x, y, z direction respectively, kinematics viscosity of hybrid nanofluid and kinematics viscosity of nanofluid are represented by ν_{hnf} and ν_{nf} .

Similarity Transformations [21]

$$p = p_0 e^{\frac{x+y}{l}} f^1(\eta),\ q = p_0 e^{\frac{x+y}{l}} g^1(\eta),$$
$$r = -(\frac{p_0 \nu}{2l})^{0.5} e^{\frac{x+y}{l}} [(f(\eta) + g(\eta)) + \eta(f^1(\eta) + (g^1(\eta)],\ \eta = (\frac{p_0}{2\nu l})^{0.5} z e^{\frac{x+y}{l}}, \quad (6)$$
$$\theta(\eta) = \frac{T - T_\infty}{T_w - T_\infty}.$$

As in the above Temperature of the fluid outside the boundary layer(K)cis represented by T_∞ and Temperature at the wall(K) is represented by T_w where T is the temperature in both states.

The subsequent ordinary equations are acquired from adopted similarity transformations from Eq. (6).

$$\frac{V_1}{V_2}(1 + \frac{1}{\beta})f^{111} + \frac{V_1}{V_2}\lambda 1 f^{11} f^{111} - \frac{V_3 V_4}{V_2} M1 f^1 + f f^{11} + g f^{11} - 2(f^1)^2 - 2 f^1 g^1 = 0, \quad (7)$$

$$\frac{V_1}{V_2}(1 + \frac{1}{\beta})g^{111} + \frac{V_1}{V_2}\lambda 1 g^{11} g^{111} - \frac{V_3 V_4}{V_2} M1 f^1 + g g^{11} + f g^{11} - 2(g^1)^2 - 2 f^1 g^1 = 0, \quad (8)$$

$$Pr[f^1\theta + g^1\theta - \theta^1 f - \theta^1 g] = \frac{V_9}{V_{10}}\theta^{11} + \frac{Ra}{V_{10}}[3(1 + (\theta_w - 1)\theta)^2(\theta_w - 1)(\theta^1)^2] + \frac{Ra}{V_{10}}[((1 + (\theta_w - 1)\theta)^3\theta^{11}] + Pr[Nt(\theta^1)^2]. \quad (9)$$

Boundary Conditions

$$f(0) = -A, g(0) = 0, f^1(0) = 1,\ g^1(0) = \alpha,$$
$$\theta^1(0) = -\frac{V_{10}}{V_9}(P_e)_T\big(1 - \theta(0)\big), \quad (10)$$
$$f^1(\eta) \to 0, g^1(\eta) \to 0, \theta(\eta) \to 0, as\ \eta \to \infty.$$

The above is the derivation for the subsequent ordinary equations is acquired from adopted similarity transformation where f, g are dimensionless stream functions, β represents casson parameter, f^1 and g^1 in the equation represents dimensionless velocity and A gives a suction or injunction parameter and Pr is the Prandt number.

Where

$$\alpha = \frac{q_0}{p_0}, M1 = \frac{2\sigma_f (B_0)^2 l}{\rho_f}, Pr = \frac{\nu_f}{\alpha_f}, Ra = \frac{16\sigma^* (T_\infty)^3}{k^* k_f},$$
$$Nt = \frac{D_T}{T_\infty}\frac{\Delta T}{\nu_f},\ \alpha_f = \frac{k_f}{(\rho c_p)_f}, (P_e)_T = \frac{\sqrt{2vlp_0}}{\alpha_f}, \theta_w = \frac{T_w}{T_\infty},$$
$$V_1 = \frac{1}{(1-\phi_{SWCNT})^{2.5}(1-\phi_{MWCNT})^{2.5}},$$
$$V_2 = (1-\phi_{SWCNT})(1-\phi_{MWCNT}) + \frac{1}{\rho_f}[\phi_{SWCNT}\rho_{SWCNT} + \phi_{MWCNT}\rho_{MWCNT}],$$
$$V_3 = 1 + \frac{3(\sigma_{MWCNT}-\sigma_f)\phi_{MWCNT}}{(\sigma_{MWCNT}+2\sigma_f)-(\sigma_{MWCNT}-\sigma_f)\phi_{SWCNT}},$$
$$V_4 = 1 + \frac{3(\sigma_{SWCNT}-V_3\sigma_f)\phi_{SWCNT}}{(\sigma_{SWCNT}+2V_3\sigma_f)-(\sigma_{SWCNT}-V_3\sigma_f)\phi_{MWCNT}},$$
$$V_5 = \frac{V_3 V_4}{V_2}, V_6 = \frac{V_1}{V_2}, \quad (11)$$
$$V_7 = \frac{(1-\phi_{MWCNT})(K_{MWCNT}-K_f)+2\phi_{MWCNT}K_{MWCNT}ln(\frac{K_{MWCNT}+K_f}{2K_f})}{(1-\phi_{MWCNT})(K_{MWCNT}-K_f)+2\phi_{MWCNT}K_f ln(\frac{K_{MWCNT}+K_f}{2K_f})},$$
$$V_8 = \frac{(1-\phi_{SWCNT})(K_{SWCNT}-V_7K_f)+2\phi_{MWCNT}K_{SWCNT}ln(\frac{K_{SWCNT}+K_fV_7}{2K_fV_7})}{(1-\phi_{SWCNT})(K_{SWCNT}-V_7K_f)+2\phi_{SWCNT}K_fV_7 ln(\frac{K_{MWCNT}+V_7K_f}{V_7 2K_f})},$$
$$V_9 = V_7V_8$$
$$V_{10} = (1-\phi_{SWCNT})(1-\phi_{MWCNT}) + \frac{\phi_{MWCNT}(\rho c_p)_{MWCNT}+\phi_{SWCNT}(\rho c_p)_{SWCNT}}{(\rho c_p)_f}.$$

Given in the equation the abbreviations like α gives the ratio of stretching rate parameter, Nt means thermophoresis parameter, K_f which is thermal conductivity of fluid, the SWCNT volume fraction and MWCNT volume fraction stands for ϕ_{SWCNT} and ϕ_{MWCNT} respectively, here σ it represents the electrical conductivity and ρ stands for density. The basic K represents the thermal conductivity of SWCNT (single wall carbon nanotube) and MWCNT (multi wall carbon nanotube).

Engineering Parameters

$$C_{fx} = \frac{\tau_{wx}}{\frac{1}{2}\rho_{hnf}p_w^2}, C_{fy} = \frac{\tau_{wy}}{\frac{1}{2}\rho_{hnf}p_w^2},$$
$$\tau_{wx} = \mu_{hnf}[\frac{\partial p}{\partial z} + \frac{\tau}{\sqrt{2}}(\frac{\partial p}{\partial z})^2]_{z=0}, \tau_{wy} = \mu_{hnf}[\frac{\partial q}{\partial z} + \frac{\tau}{\sqrt{2}}(\frac{\partial q}{\partial z})^2]_{z=0},$$
$$Nu_x = \left[-\frac{\sqrt{2}l}{(T_w-T_\infty)e^{\frac{x+y}{2l}}}\right]\left[\frac{\partial T}{\partial z} - \frac{q_r}{k_{hnf}}\right]_{z=0},$$
$$q_r = -\frac{16\sigma^* T_\infty^3}{3k^*}\frac{\partial T}{\partial z}, C_{fx}(2Re_x)^{(0.5)} = \frac{V_1}{V_2}[f^{11}(0) + \frac{\lambda 1}{2}(f^{11}(0))^2], \quad (12)$$
$$\frac{p_w}{q_w}C_{fy}(2Re_x)^{(0.5)} = \frac{V_1}{V_2}[g^{11}(0) + \frac{\lambda 1}{2}(g^{11}(0))^2],$$
$$Nu_x Re_x^{(-0.5)} = -\left(1 + \frac{Ra}{V_9}\right)\theta^1(0)\ where\ Re_x = \frac{lp_w}{\nu_f}.$$

The C_{fx} and C_{fy} explains about skin friction coefficient and $\lambda 1$ represents the Williamson's parameter, as known k_{hnf} is thermal conductivity of hybrid nanofluid.

Spatial Mathematical Modelling for Entropy Generation

$$s_{gen} = \frac{K_{hnf}}{{T_\infty}^2}\left[\left(\frac{\partial T}{\partial x}\right)^2 + \left(\frac{\partial T}{\partial y}\right)^2 + \left(\frac{\partial T}{\partial z}\right)^2\right] + \frac{\mu_{hnf}}{T_\infty}\left[2\left(\frac{\partial p}{\partial x}\right)^2 + 2\left(\frac{\partial q}{\partial y}\right)^2 + \left(\frac{\partial p}{\partial y} + \frac{\partial q}{\partial x}\right)^2\right]. \quad (13)$$

The dimensionless entropy generation of the spatial mathematical model has been deduced from the similarity variables can be written as

$$S_{gen} = (V7)(V8)[2(\eta\theta^1 + \theta)^2 + 2Re_x(\theta^1)^2] + (V1)(\chi)[(f^1 + \frac{\eta}{2}f^{11})^2 + (g^1 + \frac{\eta}{2}g^{11})^2 + \frac{1}{2}\left(f^1 + g^1 + \frac{\eta}{2}(f^{11} + g^{11})\right)^2]. \quad (14)$$

Where

$$S_{gen} = \frac{4s_{gen}{T_\infty}^2 l^2}{K_f e^{\frac{x+y}{l}}(\Delta T)^2}, \chi = \frac{8{p_w}^2 T_\infty \mu_f}{K_f(\Delta T)^2}, Re_x = \frac{l p_w}{\nu_f}. \quad (15)$$

Specifically, Sgen is the rate of entropy generation, χ is the irreversibility factor, and Rex is the local Reynolds number.

3. Results and Discussion

The methodology of this theme is to examine the properties of hybrid carbon nanotubes on Williamson nanofluid over a stretching sheet. Numerical and computer simulations are done with python with bvp solver to obtain the solutions using Runge Kutta method. Investigators estimated the asymptotic solutions of boundary conditions using shooting techniques. The cause and effect of thermophysical properties of SWCNT, MWCNT, and hybrid carbon nanotubes of momentum and thermal boundary layers are portrayed and discussed. Majority of related literature has been emphasised on Williamson fluid parameter ($\lambda 1$), Magnetic parameter(M1), thermophoretic parameter (Nt) , and Brownian motion parameter (Nb) , Prandtl number (Pr), Schmidt number (Sc), radiation parameter(Ra),temperature ratio (θ_w), Casson parameter(β), but only few literature studies are available on thermal Peclet number (Pe_T) . The influence of thermal Peclet number (Pe_T) of nanofluids explored with hybrid carbon nanotubes equipped with nonlinear radiation has been investigated. The threshold values of thermo physical parameters are adopted to get the convergence of boundary layers at η=10 having Δη=0.01. The erected model is validated with the suitable comparative study as interpreted in Table 1.

Table 1
Validations of numerical assessment at Pr=0.5, Nb=0.5, Nt=0.5, and Sc=1.0

λ1	A	M1	$-(f^{11}(0) + \frac{\lambda_1}{2}(f^{11}(0))^2)$	
			Ahmed and Akbar [21]	Present
0.1	0.2	2.0	1.754213	1.7542216
hq0.2	0.2	2.0	1.678675	1.6786912
0.3	0.2	2.0	1.579827	1.579827

Figure 2 represents the thermal boundary layer with the effect of thermal Peclet number (Pe_T). It is further identified that an increasing thermal Peclet number leads the temperature profiles at the wall. It is concluded that the fluid temperature near the stretching sheet's wall is influenced by increases in enthalpy because of adopted boundary conditions.

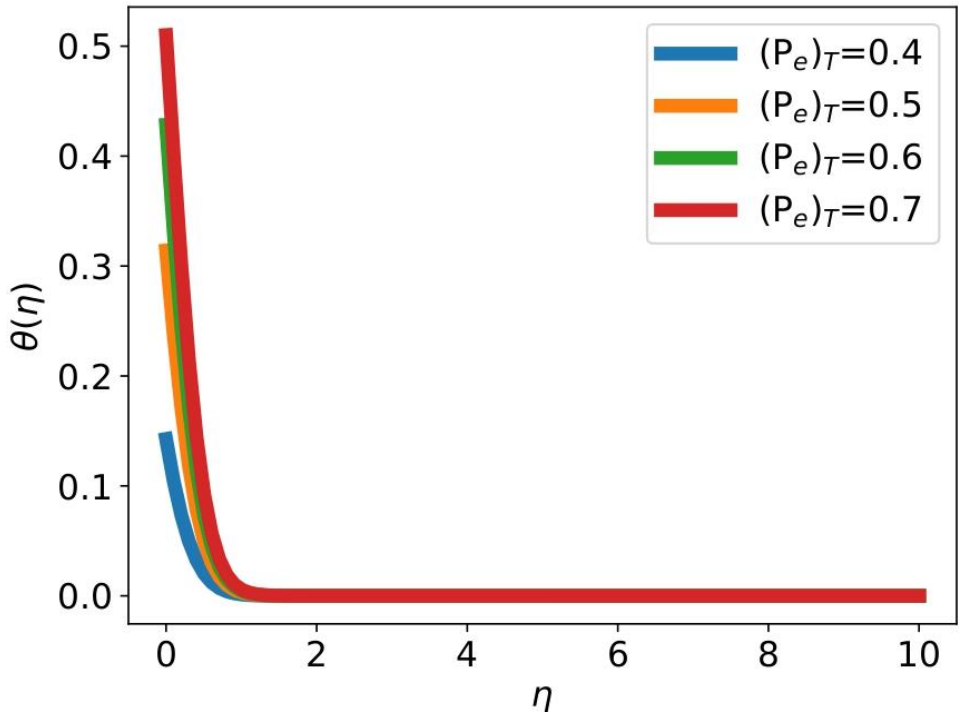

Fig. 2. Influence of thermal Peclet number (Pe_T) on temperature profile

Figure 3 to Figure 8 depicts the momentum, temperature, and entropy generation of base fluids with SWCNT, MWCNT and hybrid CNTs at boundary layer of stretching sheet. Velocity of fluid with hybrid particles exhibits dominated role with the aid of SWCNT, and MWCNT as portrayed in Figure 3. We can observe the same impact on vertical velocity as shown in Figure 4. Temperature of the fluid explored with MWCNT plays a vital role with respect to SWCNT and hybrid particles as depicted in Figure 5. We can conclude that a thermo-physical property of base fluids with MWCNT is the major impact to raise the temperature near the wall. Rate of entropy is dominated by water explored with hybrid CNTs as revealed in Figure 6. We observed the impact of Casson parameter (β) and Williamson fluid parameter ($\lambda 1$) on the rate of entropy generation as portrayed in Figure 7 and Figure 8 respectively. Reduction of entropy generation takes place with enhancing $\lambda 1$ and β, but reverse tendency occurs with rise of β when base fluid explored with hybrid particles.

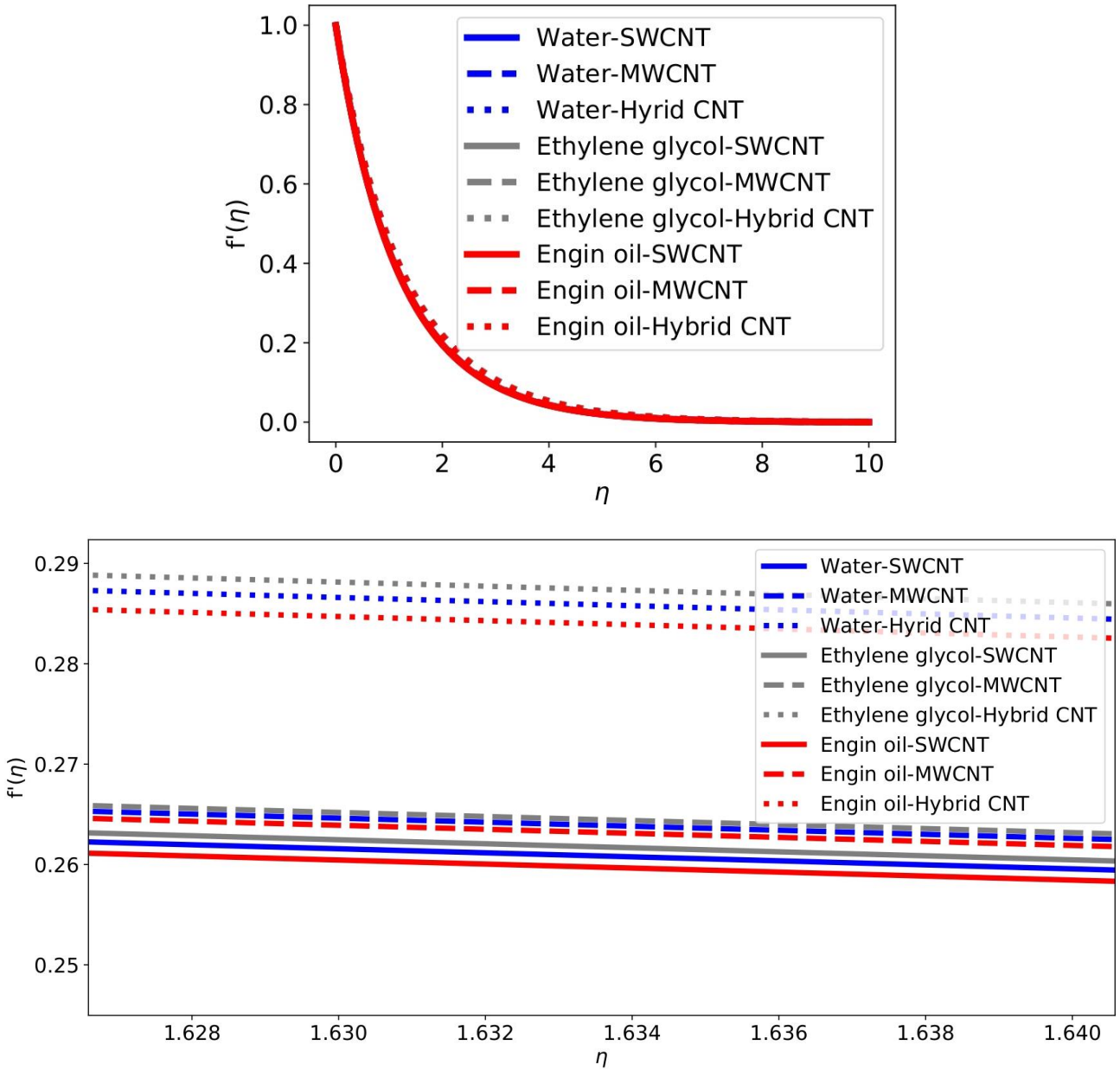

Fig. 3. Influence of different base fluids explored with CNT on horizontal velocity profile

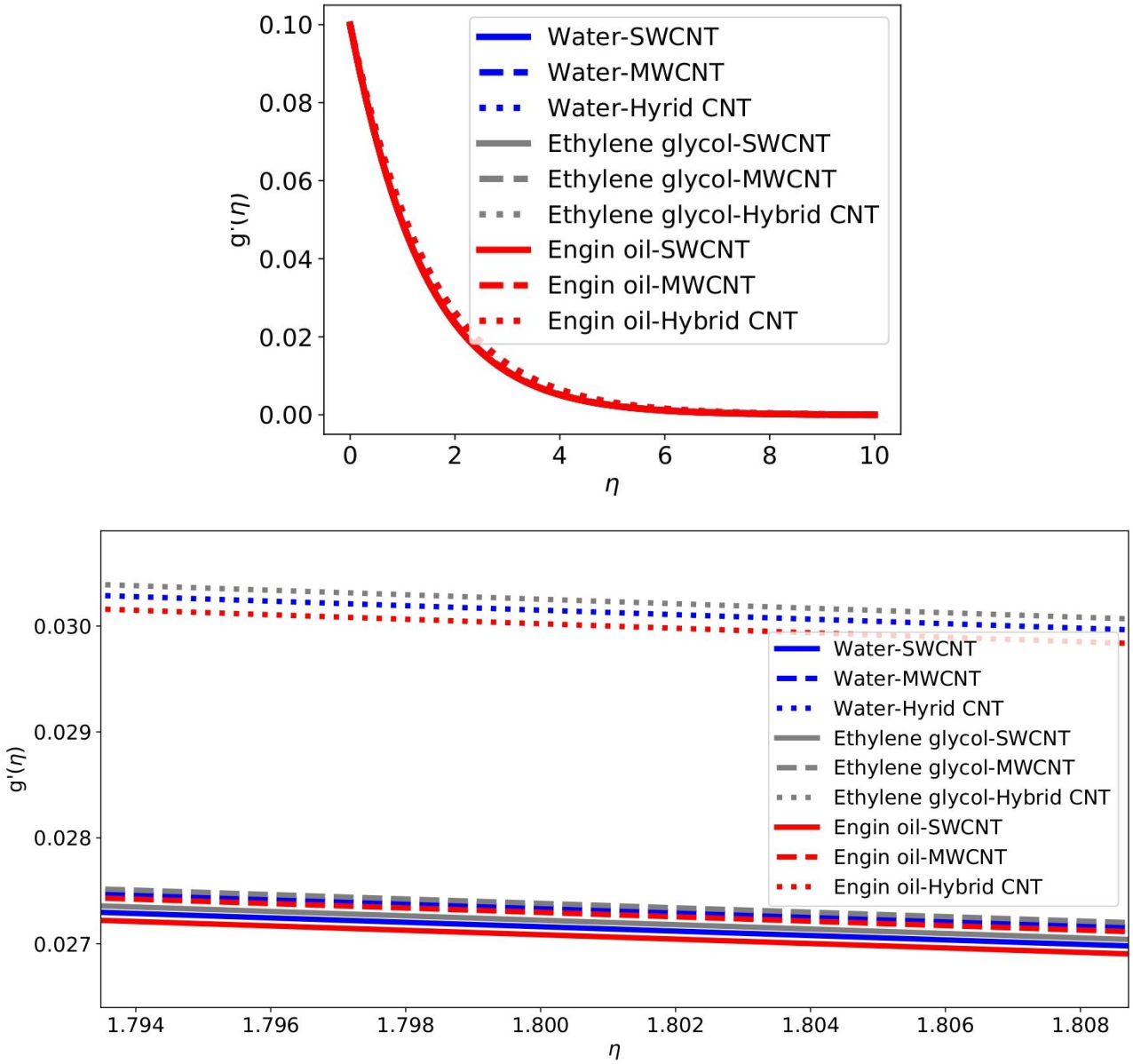

Fig. 4. Influence of different base fluids explored with CNT on vertical velocity profile

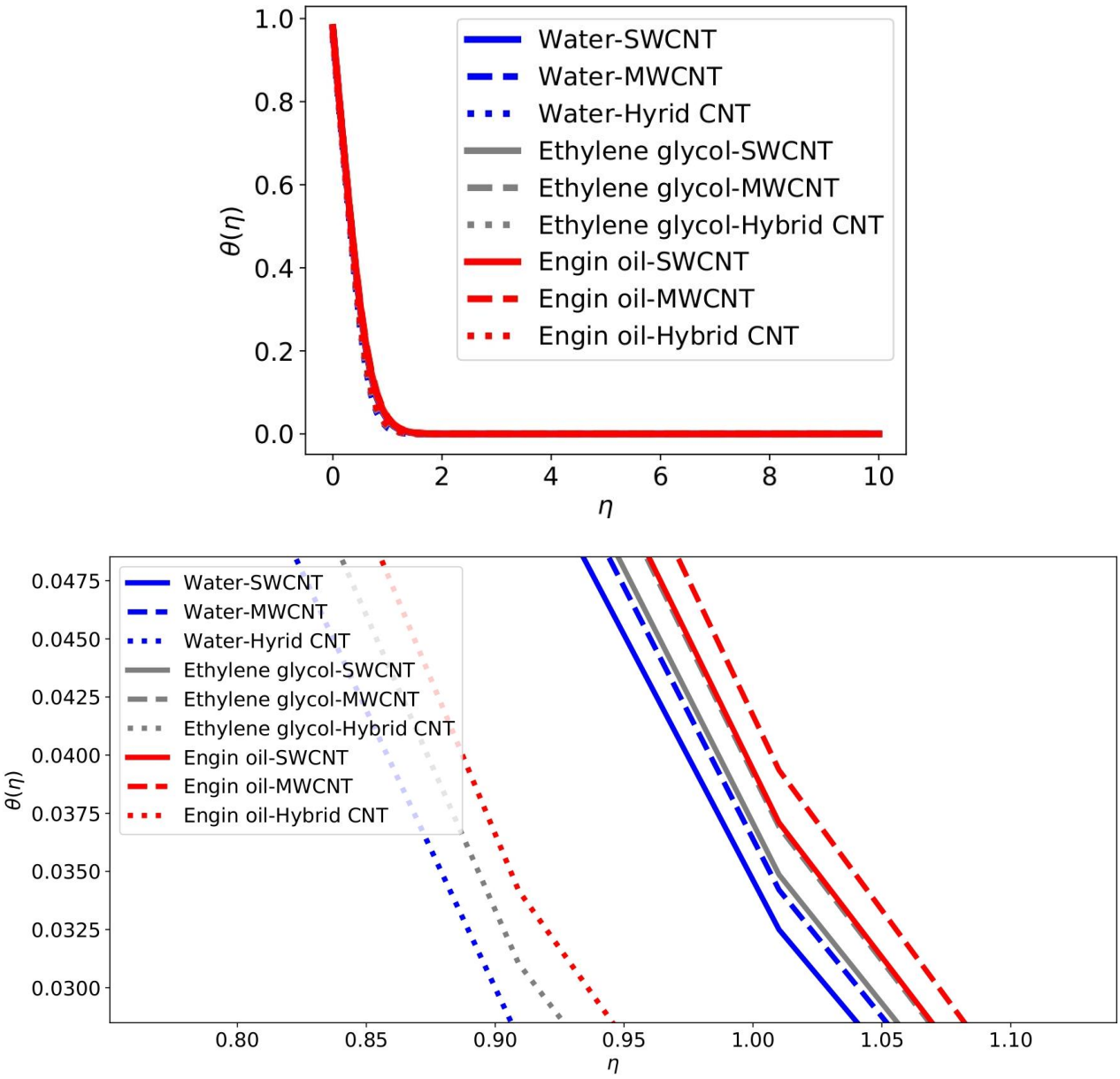

Fig. 5. Influence of different base fluids explored with CNT on temperature profile

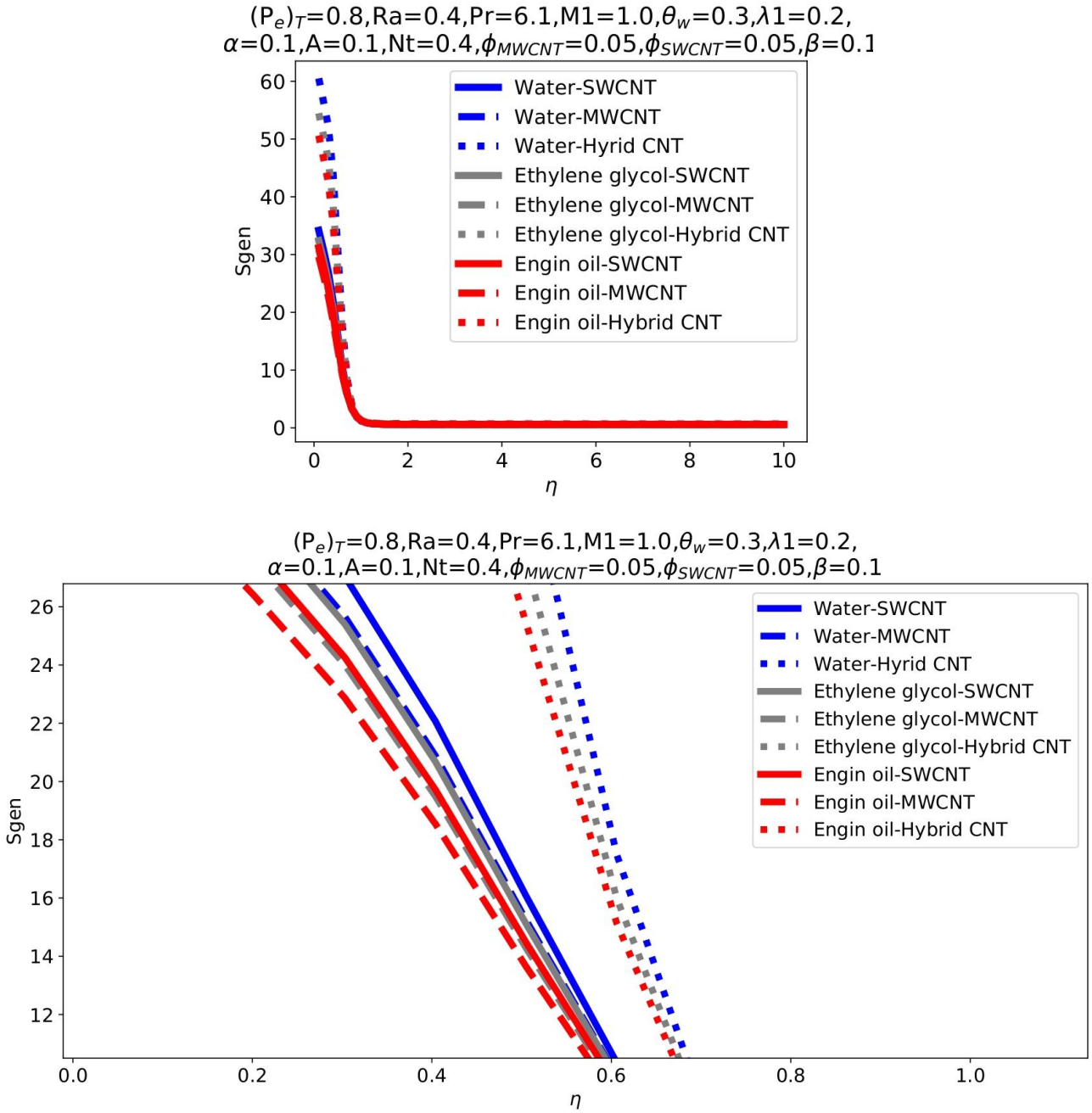

Fig. 6. Influence of different base fluids explored with CNT on the rate of entropy

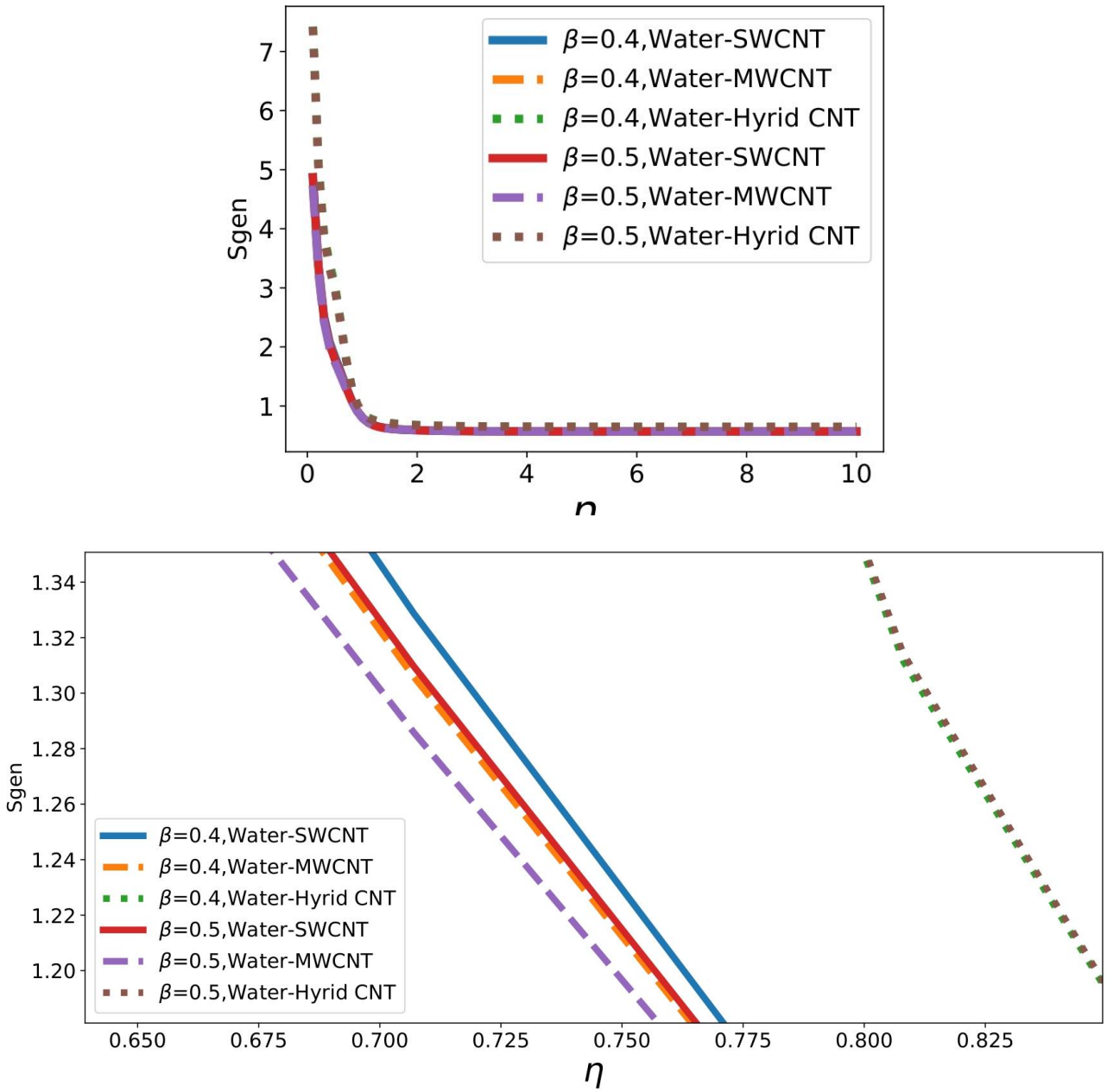

Fig. 7. Influence of Casson parameter (β) on the rate of entropy with differed CNTs

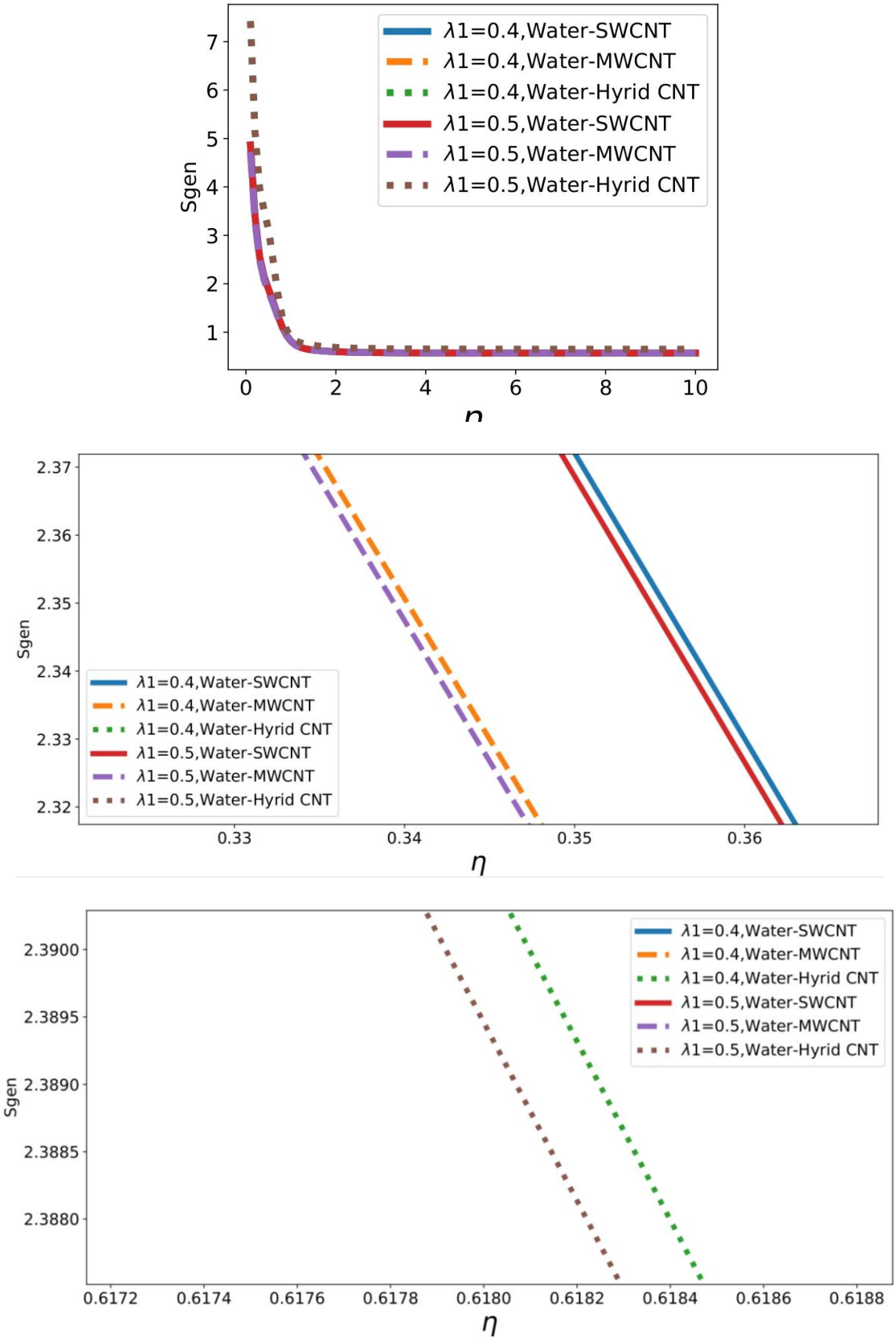

Fig. 8. Influence of Williamson's parameter (λ1) on the rate of entropy with differed CNTs

Table 2 and Table 3 shows horizontal, vertical Skin friction and Nusselt number are downtrends with increasing M1, and β. Horizontal and vertical Skin friction is uptrend with enhancing λ1 can be

observed from Table 4, but in contrast Nusselt number decreases. We watched the rate of heat transfer from fluid to sheet near the wall decreases with enhancing M1, β, and$\lambda 1$. We can conclude that the resistivity is the main cause for heat transfer.

Table 2
Influence of M1, β, and λ1 on $(2Rex)^{0.5}cf_x$ at Pr=6.1, Ra=0.4, θw=0.3, Nt=0.4, α=0.1, A=0.1, Pe_T =0.8

		M1=1	M1=2	M1=3	M1=4
Water	SWCNT	-0.767856	-0.880695	-0.979353	-1.06786
	MWCNT	-0.793639	-0.793639	-1.01894	-1.11284
	Hybrid CNT	-0.797229	-0.908016	-1.00558	-1.09354
Ethylene glycol	SWCNT	-0.774493	-0.889218	-0.989439	-1.0793
	MWCNT	-0.798081	-0.91976	-1.02572	-1.12054
	Hybrid CNT	-0.807938	-0.921673	-1.02171	-1.1118
Engine oil	SWCNT	-0.759752	-0.870302	-0.967061	-1.05392
	MWCNT	-0.788167	-0.906984	-1.01058	-1.10336
	Hybrid CNT	-0.784342	-0.891613	-0.986238	-1.07163
		β =0.1	β =0.2	β =0.3	β =0.4
Water	SWCNT	-0.56198	-0.753024	-0.880695	-0.976001
	MWCNT	-0.583092	-0.781444	-0.914034	-1.01303
	Hybrid CNT	-0.578943	-0.77611	-0.908016	-1.00652
Ethylene glycol	SWCNT	-0.567376	-0.760289	-0.889218	-0.985468
	MWCNT	-0.586717	-0.786325	-0.91976	-1.01939
	Hybrid CNT	-0.587585	-0.787747	-0.921673	-1.02169
Engine oil	SWCNT	-0.555402	-0.744167	-0.870302	-0.964459
	MWCNT	-0.578629	-0.775435	-0.906984	-1.0052
	Hybrid CNT	-0.568563	-0.762133	-0.891613	-0.988299
		λ1 =0.1	λ1 =0.2	λ1 =0.3	λ1 =0.4
Water	SWCNT	-0.880695	-0.84562	-0.809589	-0.772538
	MWCNT	-0.914034	-0.878052	-0.841099	-0.803113
	Hybrid CNT	-0.908016	-0.874501	-0.840138	-0.804876
Ethylene glycol	SWCNT	-0.889218	-0.853923	-0.817667	-0.780389
	MWCNT	-0.91976	-0.883629	-0.846525	-0.808385
	Hybrid CNT	-0.921673	-0.887839	-0.853155	-0.817569
Engine oil	SWCNT	-0.870302	-0.835497	-0.799738	-0.762962
	MWCNT	-0.906984	-0.871186	-0.83442	-0.796622
	Hybrid CNT	-0.891613	-0.858478	-0.8245	-0.789628

Table 3
Influence of M1, β, and λ1 on $(2Rex)^{0.5}cf_y$ at Pr=6.1, Ra=0.4, θw=0.3, Nt=0.4, α=0.1, A=0.1, Pe_T =0.8

		M1=1	M1=2	M1=3	M1=4
Water	SWCNT	-0.055944	-0.072023	-0.085107	-0.096426
	MWCNT	-0.058293	-0.075292	-0.089095	-0.101023
	Hybrid CNT	-0.057141	-0.073082	-0.086114	-0.097413
Ethylene glycol	SWCNT	-0.056541	-0.07285	-0.086116	-0.097588
	MWCNT	-0.058694	-0.07585	-0.089775	-0.101807
	Hybrid CNT	-0.058091	-0.074396	-0.087715	-0.099256
Engine oil	SWCNT	-0.055217	-0.071014	-0.083879	-0.095012
	MWCNT	-0.057798	-0.074605	-0.088259	-0.10006
	Hybrid CNT	-0.056001	-0.071506	-0.084196	-0.095203
		β =0.1	β =0.2	β =0.3	β =0.4
Water	SWCNT	-0.04555	-0.061383	-0.072023	-0.079972
	MWCNT	-0.047604	-0.064161	-0.075292	-0.083609
	Hybrid CNT	-0.046236	-0.062284	-0.073082	-0.08115
Ethylene glycol	SWCNT	-0.04607	-0.062086	-0.07285	-0.080892
	MWCNT	-0.047955	-0.064636	-0.07585	-0.084229
	Hybrid CNT	-0.047062	-0.063402	-0.074396	-0.082612
Engine oil	SWCNT	-0.044916	-0.060526	-0.071014	-0.07885
	MWCNT	-0.047173	-0.063578	-0.074605	-0.082845
	Hybrid CNT	-0.045244	-0.060944	-0.071506	-0.079396
		λ1 =0.1	λ1 =0.2	λ1 =0.3	λ1 =0.4
Water	SWCNT	-0.072023	-0.071802	-0.07158	-0.071358
	MWCNT	-0.075292	-0.075062	-0.074832	-0.074601
	Hybrid CNT	-0.073082	-0.072875	-0.072668	-0.07246
Ethylene glycol	SWCNT	-0.07285	-0.072627	-0.072404	-0.07218
	MWCNT	-0.07585	-0.075619	-0.075387	-0.075155
	Hybrid CNT	-0.074396	-0.074186	-0.073976	-0.073765
Engine oil	SWCNT	-0.071014	-0.070796	-0.070577	-0.070358
	MWCNT	-0.074605	-0.074377	-0.074149	-0.07392
	Hybrid CNT	-0.071506	-0.071302	-0.071099	-0.070895

Table 4
Influence of M1, β, and λ1 on $(2Re_x)^{0.5}Nu_x$ at Pr=6.1, Ra=0.4, θw=0.3, Nt=0.4, α=0.1, A=0.1, Pe_T =0.8

		M1=1	M1=2	M1=3	M1=4
Water	SWCNT	1.85363	1.84502	1.83743	1.83056
	MWCNT	1.86946	1.86024	1.85215	1.84483
	Hybrid CNT	1.7078	1.70379	1.70024	1.69703
Ethylene glycol	SWCNT	1.87045	1.86123	1.85313	1.84579
	MWCNT	1.88759	1.87772	1.869	1.86116
	Hybrid CNT	1.73198	1.72737	1.72334	1.71967
Engine oil	SWCNT	1.8807	1.87112	1.86261	1.85494
	MWCNT	1.89876	1.8884	1.87929	1.87105
	Hybrid CNT	1.74802	1.74299	1.73857	1.73454
		β =0.1	β =0.2	β =0.3	β =0.4
Water	SWCNT	1.86757	1.85415	1.84502	1.8381
	MWCNT	1.88379	1.86978	1.86024	1.85302
	Hybrid CNT	1.71488	1.70828	1.70379	1.70039
Ethylene glycol	SWCNT	1.88519	1.87094	1.86123	1.85389
	MWCNT	1.9028	1.88786	1.87772	1.86997
	Hybrid CNT	1.73992	1.73245	1.72737	1.72355
Engine oil	SWCNT	1.89637	1.88132	1.87112	1.86331
	MWCNT	1.91494	1.89918	1.8884	1.88025
	Hybrid CNT	1.757	1.74866	1.74299	1.73872
		λ1 =0.1	λ1 =0.2	λ1 =0.3	λ1 =0.4
Water	SWCNT	1.84502	1.84466	1.84429	1.8439
	MWCNT	1.86024	1.85987	1.85949	1.8591
	Hybrid CNT	1.70379	1.70362	1.70344	1.70326
Ethylene glycol	SWCNT	1.86123	1.86085	1.86046	1.86006
	MWCNT	1.87772	1.87733	1.87692	1.87646
	Hybrid CNT	1.72737	1.72718	1.72699	1.72678
Engine oil	SWCNT	1.87112	1.87072	1.87031	1.86988
	MWCNT	1.8884	1.88799	1.88756	1.88712
	Hybrid CNT	1.74299	1.74277	1.74257	1.74234

We can identify the fact that heat transfer rate from fluid to sheet near the wall enhances with levitate the radiation (Ra), temperature ratio (θw), and thermal Peclet number (Pe_T) as shown from Table 5 and Table 6, but opposite behavior was identified with enhancing the value of thermophoretic parameter (Nt), because of less emissivity.

Table 5
Influence of Ra and θ_w on $(2Re_x)^{0.5}Nu_x$ at Pr=6.1, λ1 =0.1, β=0.3, M1=1.0, Nt=0.4, α=0.1, A=0.1, Pe_T=0.8

		Ra=0.1	Ra=0.2	Ra=0.3	Ra=0.4
Water	SWCNT	1.56467	1.65682	1.83743	1.84502
	MWCNT	1.56777	1.66392	1.85215	1.86024
	Hybrid CNT	1.53395	1.58965	1.70024	1.70379
Ethylene glycol	SWCNT	1.56753	1.6641	1.85313	1.86123
	MWCNT	1.57065	1.67163	1.869	1.87772
	Hybrid CNT	1.54082	1.60204	1.72334	1.72737
Engine oil	SWCNT	1.5686	1.6681	1.86261	1.87112
	MWCNT	1.57177	1.67595	1.87929	1.8884
	Hybrid CNT	1.54475	1.60985	1.73857	1.73454
		θ_w =0.1	θ_w =0.2	θ_w =0.3	θ_w =0.4
Water	SWCNT	1.82088	1.83268	1.84502	1.85545
	MWCNT	1.83628	1.84803	1.86024	1.87048
	Hybrid CNT	1.67855	1.69057	1.70379	1.71577
Ethylene glycol	SWCNT	1.8375	1.84915	1.86123	1.87134
	MWCNT	1.85421	1.86577	1.87772	1.88754
	Hybrid CNT	1.7024	1.71434	1.72737	1.73917
Engine oil	SWCNT	1.84792	1.85932	1.87112	1.8808
	MWCNT	1.8656	1.8769	1.8884	1.89782
	Hybrid CNT	1.71874	1.73036	1.74299	1.75431

Table 6
Influence of Nt, and $(Pe)_T$ on $(2Re_x)^{0.5}Nu_x$ at Pr=6.1, λ1 =0.1, β=0.3, M1=1.0, Ra=0.4, α=0.1, A=0.1, θ_w=0.2

		Nt=0.1	Nt=0.2	Nt=0.3	Nt=0.4
Water	SWCNT	3.23757	2.5287	2.11219	1.84502
	MWCNT	3.23334	2.54123	2.12787	1.86024
	Hybrid CNT	3.28789	2.39293	1.95997	1.70379
Ethylene glycol	SWCNT	3.22687	2.54008	2.12838	1.86123
	MWCNT	3.22079	2.55254	2.14495	1.87772
	Hybrid CNT	3.28132	2.41929	1.98639	1.72737
Engine oil	SWCNT	3.21102	2.54365	2.1373	1.87112
	MWCNT	3.20304	2.55581	2.15441	1.8884
	Hybrid CNT	3.26146	2.4326	2.00301	1.74299
		$(Pe)_T$ =0.1	$(Pe)_T$ =0.2	$(Pe)_T$ =0.3	$(Pe)_T$ =0.4
Water	SWCNT	-2.81408	0.214145	1.0434	1.32789
	MWCNT	-2.59507	0.354257	1.10664	1.36873
	Hybrid CNT	-3.45953	-2.54214	-0.536106	0.468916
Ethylene glycol	SWCNT	-2.54769	0.383861	1.11867	1.3756
	MWCNT	-2.29135	0.516767	1.18016	1.41665
	Hybrid CNT	-3.67681	-1.91627	-0.024688	0.746278
Engine oil	SWCNT	-2.32429	0.503745	1.1711	1.40859
	MWCNT	-2.03842	0.632034	1.2319	1.45013
	Hybrid CNT	-3.81522	-1.39031	0.302698	0.913289

4. Conclusions

The investigation concluded that behavior of Williamson nanofluid explored with various CNTs under the consideration of thermo-physical properties such as nonlinear radiation parameter and thermal Peclet number (Pe_T) within the whole domain [0.0, 2.0]. The following outcomes are generated:

(i) Temperature of fluid nearer to the surface increases with increasing thermal Peclet number (Pe_T).

(ii) Velocity of Ethylene glycol explored with hybrid CNTs is enhanced
(iii) Thermal distribution of Engine oil explored with MWCNT near the surface is henpecked
(iv) Concentration of Engine oil explored with SWCNT is widened
(v) Coefficient of local Nusselt number increase with enhancing Williamsons parameter (λ1)
(vi) As radiation parameter and temperature ratio increase, heat flux rate also increases.
(vii) Rate of entropy of water explored with hybrid CNTs is magnified.
(viii) Rate of entropy decays for augmented values of Williamson parameter (λ1).
(ix) Rate of entropy of fluid with SWCNT and MWCNT decays for augmented values of Williamson parameter (λ1), but reverse tendency occurs at fluid with hybrid CNT.

Models along stretched sheets with carbon nanotubes and hybrid carbon nanotubes show that deformation of fluid near the boundary layer is influenced by the thermal Peclet number, so it is important to simulate heat transfer rates before conducting practical experiments.

Acknowledgement
The investigators are extremely thankful to Koneru Lakshmaiah Education Foundation and Jawaharlal Nehru architecture and fine arts university for providing a whole lot of support to this research project at the department of mathematics, Koneru Lakshmaiah Education Foundation, Guntur, and the department of digital technology, Jawaharlal Nehru architecture and fine arts university, Hyderabad.

References

[1] Modather, M., A. M. Rashad, and A. J. Chamkha. "An analytical study of MHD heat and mass transfer oscillatory flow of a micropolar fluid over a vertical permeable plate in a porous medium." *Turkish Journal of Engineering and Environmental Sciences* 33, no. 4 (2009): 245-258.
[2] Chamkha, Ali J., A. S. Dogonchi, and D. D. Ganji. "Magnetohydrodynamic nanofluid natural convection in a cavity under thermal radiation and shape factor of nanoparticles impacts: a numerical study using CVFEM." *Applied Sciences* 8, no. 12 (2018): 2396. https://doi.org/10.3390/app8122396
[3] Dogonchi, A. S., Seyyed Masoud Seyyedi, M. Hashemi-Tilehnoee, Ali J. Chamkha, and D. D. Ganji. "Investigation of natural convection of magnetic nanofluid in an enclosure with a porous medium considering Brownian motion." *Case Studies in Thermal Engineering* 14 (2019): 100502. https://doi.org/10.1016/j.csite.2019.100502
[4] Krishna, M. Veera, and Ali J. Chamkha. "Hall and ion slip effects on MHD rotating boundary layer flow of nanofluid past an infinite vertical plate embedded in a porous medium." *Results in Physics* 15 (2019): 102652. https://doi.org/10.1016/j.rinp.2019.102652
[5] Krishna, M. Veera, and Ali J. Chamkha. "Hall effects on MHD squeezing flow of a water-based nanofluid between two parallel disks." *Journal of Porous Media* 22, no. 2 (2019): 209-223. https://doi.org/10.1615/JPorMedia.2018028721
[6] Krishna, M. Veera, and Ali J. Chamkha. "Hall and ion slip effects on Unsteady MHD Convective Rotating flow of Nanofluids-Application in Biomedical Engineering." *Journal of the Egyptian Mathematical Society* 28, no. 1 (2020): 1. https://doi.org/10.1186/s42787-019-0065-2
[7] Krishna, M. Veera, N. Ameer Ahamad, and Ali J. Chamkha. "Hall and ion slip effects on unsteady MHD free convective rotating flow through a saturated porous medium over an exponential accelerated plate." *Alexandria Engineering Journal* 59, no. 2 (2020): 565-577. https://doi.org/10.1016/j.aej.2020.01.043
[8] Dogonchi, A. Sattar, M. S. Sadeghi, M. Ghodrat, Ali J. Chamkha, Yasser Elmasry, and Radi Alsulami. "Natural convection and entropy generation of a nanoliquid in a crown wavy cavity: effect of thermo-physical parameters and cavity shape." *Case Studies in Thermal Engineering* 27 (2021): 101208. https://doi.org/10.1016/j.csite.2021.101208
[9] Dogonchi, A. Sattar, S. R. Mishra, Ali J. Chamkha, M. Ghodrat, Yasser Elmasry, and Hesham Alhumade. "Thermal and entropy analyses on buoyancy-driven flow of nanofluid inside a porous enclosure with two square cylinders: Finite element method." *Case Studies in Thermal Engineering* 27 (2021): 101298. https://doi.org/10.1016/j.csite.2021.101298

[10] Hamrelaine, Salim, Fateh Mebarek-Oudina, and Mohamed Rafik Sari. "Analysis of MHD Jeffery Hamel flow with suction/injection by homotopy analysis method." *Journal of Advanced Research in Fluid Mechanics and Thermal Sciences* 58, no. 2 (2019): 173-186.
[11] Khan, Ansab Azam, Khairy Zaimi, Suliadi Firdaus Sufahani, and Mohammad Ferdows. "MHD flow and heat transfer of double stratified micropolar fluid over a vertical permeable shrinking/stretching sheet with chemical reaction and heat source." *Journal of Advanced Research in Applied Sciences and Engineering Technology* 21, no. 1 (2020): 1-14. https://doi.org/10.37934/araset.21.1.114
[12] Nadeem, S., and S. T. Hussain. "Heat transfer analysis of Williamson fluid over exponentially stretching surface." *Applied Mathematics and Mechanics* 35, no. 4 (2014): 489-502. https://doi.org/10.1007/s10483-014-1807-6
[13] Kumar, K. Ganesh, N. G. Rudraswamy, B. J. Gireesha, and S. Manjunatha. "Non linear thermal radiation effect on Williamson fluid with particle-liquid suspension past a stretching surface." *Results in Physics* 7 (2017): 3196-3202. https://doi.org/10.1016/j.rinp.2017.08.027
[14] Amanulla, C. H., N. Nagendra, and M. Suryanarayana Reddy. "Numerical simulation of slip influence on the flow of a MHD Williamson fluid over a vertical convective surface." *Nonlinear Engineering* 7, no. 4 (2018): 309-321. https://doi.org/10.1515/nleng-2017-0079
[15] Lund, Liaquat Ali, Zurni Omar, and Ilyas Khan. "Analysis of dual solution for MHD flow of Williamson fluid with slippage." *Heliyon* 5, no. 3 (2019): e01345. https://doi.org/10.1016/j.heliyon.2019.e01345
[16] Kho, Yap Bing, Abid Hussanan, Muhammad Khairul Anuar Mohamed, and Mohd Zuki Salleh. "Heat and mass transfer analysis on flow of Williamson nanofluid with thermal and velocity slips: Buongiorno model." *Propulsion and Power Research* 8, no. 3 (2019): 243-252. https://doi.org/10.1016/j.jppr.2019.01.011
[17] Rasool, Ghulam, Ting Zhang, Ali J. Chamkha, Anum Shafiq, Iskander Tlili, and Gullnaz Shahzadi. "Entropy generation and consequences of binary chemical reaction on MHD Darcy-Forchheimer Williamson nanofluid flow over non-linearly stretching surface." *Entropy* 22, no. 1 (2019): 18. https://doi.org/10.3390/e22010018
[18] Dawar, Abdullah, Zahir Shah, and Saeed Islam. "Mathematical modeling and study of MHD flow of Williamson nanofluid over a nonlinear stretching plate with activation energy." *Heat Transfer* 50, no. 3 (2021): 2558-2570. https://doi.org/10.1002/htj.21992
[19] Qureshi, Muhammad Amer. "Numerical simulation of heat transfer flow subject to MHD of Williamson nanofluid with thermal radiation." *Symmetry* 13, no. 1 (2020): 10. https://doi.org/10.3390/sym13010010
[20] Goud, B. Shankar. "Boundary layer and heat transfer Williamson fluid flow over a stretching sheet with Newtonian heating." *Turkish Journal of Computer and Mathematics Education (TURCOMAT)* 12, no. 10 (2021): 1275-1280.
[21] Ahmed, Kamran, and Tanvir Akbar. "Numerical investigation of magnetohydrodynamics Williamson nanofluid flow over an exponentially stretching surface." *Advances in Mechanical Engineering* 13, no. 5 (2021): 16878140211019875. https://doi.org/10.1177/16878140211019875